The Effects of Carbonization Temperature on the Properties and Structure of PAN-Based Activated Carbon Hollow Fiber

Junfen Sun, Guangxiang Wu, Qingrui Wang

College of Material Science and Engineering, Donghua University, Yan an West Road 1882, 200051, Shanghai, People's Republic of China

Received 12 January 2004; accepted 9 August 2004
DOI 10.1002/app.21955
Published online in Wiley InterScience (www.interscience.wiley.com).

ABSTRACT: Polyacrylonitrile (PAN) hollow fibers were pretreated with ammonium dibasic phosphate and then further oxidized in air, carbonized in nitrogen, and activated with carbon dioxide. The effects of carbonization temperature of PAN hollow fiber precursor on the microstructure, specific surface, pore-size distribution, and adsorption properties of PAN-based carbon hollow fiber (PAN-CHF) and PAN-based activated carbon hollow fibers (PAN-ACHF) were studied in this work. After the activation process, the surface area of the PAN-ACHF increased very remarkably, reaching 900 $m^2\ g^{-1}$ when carbonization is 1000°C, and the adsorption ratios to creatinine and VB_{12} of ACHF were much higher than those of CHF, especially to VB_{12}. The different adsorption ratios to two adsorbates including creatinine and VB_{12} reflect the number of micropores and mesopores in PAN-ACHF. The dominant pore sizes of mesopores in PAN-ACHF are from 2 to 5 nm. © 2005 Wiley Periodicals, Inc. J Appl Polym Sci 97: 2155–2160, 2005

Key words: carbonization; polyacrylonitrile; activated carbon hollow fiber; adsorption properties

INTRODUCTION

Carbon fibers produced from rayon, polyacrylonitrile (PAN), pitch, or phenolic resin are converted by partial gasification in steam or other oxidizing gas to activated carbon fibers of high surface area.[1–3] Activated carbon fibers have higher specific surface area and more micropores developed on the surface of the fiber than granulated active carbon. Therefore, activated carbon fibers have been widely used in various areas such as water treatment,[4,5] the removal of SO_x and NO_x,[6,7] and the adsorption of toxic gases.[8,9] Recently, the PAN-based activated carbon hollow fiber (PAN-ACHF) has brought on many investigators' interest,[10–15] because PAN-ACHF shows the largest adsorption capacity among the carbon surfaces.

There have been numerous applications of hollow fiber technology to separation and purification in both industry and medicine, including the preparation of drinkable, high-quality water for the electronics and pharmaceutical industries, treatment of secondary effluent from sewage, processing plants, gas separation for industrial application, hemodialyzers, and the controlled release of drugs to mention only a few applications.[16] However, attempts to commercialize hollow fibers or other membrane systems for such separations have been unsuccessful, largely because of relatively low permeation rates and poor environmental resistance.

Yang and Yu[10–13] studied the structure and properties, pore-size distribution, surface area, and mechanical properties of PAN-ACHF. Linkov et al.[17] reported that hollow fibers have been used for gas separation and show high fluxes and good selectivities. Schindler and Maier[18] obtained a patent for making hollow carbon fiber membrane, in which the PAN hollow fiber was pretreated with hydrazine and followed by oxidation and carbonization, and was suitable for separating particles.

In this research, the PAN hollow fibers were dipped in ammonium dibasic phosphate aqueous solution, oxidized in air, carbonized in nitrogen, and activated with carbon dioxide. This study examined the effects of carbonization temperature of stabilized PAN hollow fiber precursor on the adsorption and structural properties, such as specific surface area pore size distribution and morphology of PAN-based carbon hollow fiber (PAN-CHF) and PAN-ACHF. We discuss the adsorption properties of the resultant PAN-based ACHF to creatinine and VB_{12}. Creatinine and VB_{12} are two adsorbates in this work. VB_{12} is a kind of vitamin. The molecular weight of creatinine (113) is less than that of VB_{12} (1335.5). According to their molecule sizes, creatinine $<$ VB_{12}, the molecule size of creatinine is less than 2 nm and primarily adsorbed by micropores ($<$2 nm). However, the molecule size of

Correspondence to: J. Sun (junfensun@sohu.com).

VB_{12} is larger than 2 nm and primarily adsorbed by mesopores(2–50 nm). There are various types of pores in the ACHF. Macropores have small specific surface area and are thus insignificant to adsorption. However, these pores control the access of adsorbate and also serve as the space for deposition. Mesopores provide channels for the adsorbate to the micropores from the macropores and simultaneously adsorb matter of mesomolecules. As reported in the literature, mesopore can function as capillary condensation; thus, it is indispensable for the adsorption of liquid and gas. Micropores determine the adsorption capacity of the ACHF and primarily adsorb the matter of micromolecules. It is the purpose of this article to discuss what carbonization process condition provides high surface area and high adsorption ratio for the PAN-ACHF prepared from PAN hollow fibers.

EXPERIMENTAL

PAN (a copolymer of acrylonitrile, methyl methacrylate, and itaconic acid) was supplied by China Petroleum & Chemical Corp. (Bejing, China). PAN hollow fiber spun by dry–wet spinning setup was used as the precursor. The resultant hollow fiber had an inside diameter of 400 μm and an outside diameter of 500 μm. Figure 1 shows the porous structure of the PAN hollow fiber.

Virgin PAN hollow fiber was first dipped in ammonium dibasic phosphate aqueous solution. Afterwards, the pretreated fiber was oxidized in the air, carbonized in nitrogen, and activated with carbon dioxide. The carbonization temperature is changed.

A scanning electron microscope (SEM; JEOL Model JSM-5600LV) was used to examine the cross section and external surface of fibers.

Adsorption study to creatinine and VB_{12} was carried out by a static process. A known quantity of the ACHF was immersed in a known volume of aqueous solution at 37°C for 24 h. The amount of creatinine and VB_{12} adsorbed was determined by the concentration

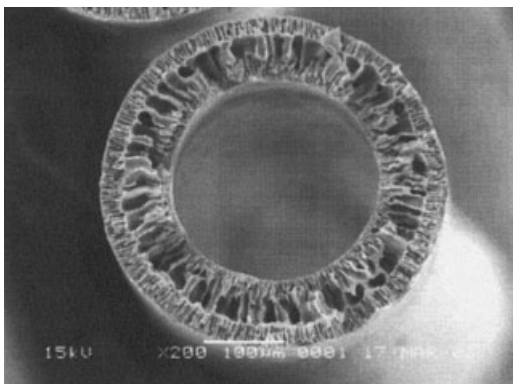

Figure 1 The cross section of virgin PAN hollow fiber (×200).

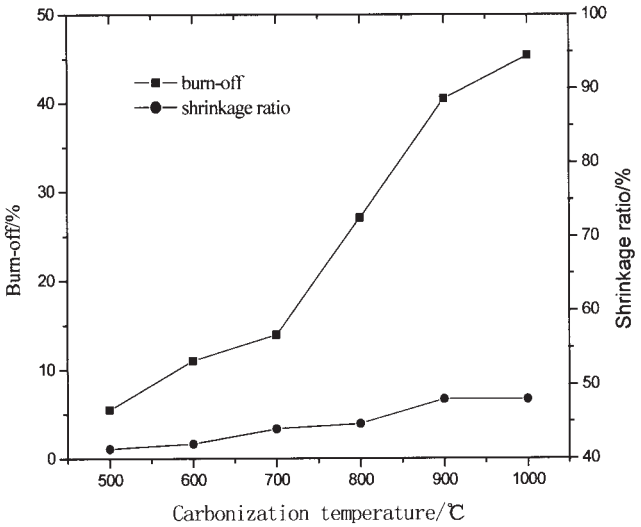

Figure 2 Burn-off and shrinkage ratio of PAN-CHF versus carbonization temperature. [The samples are pretreated with ammonium dibasic phosphate of 4% (wt %) concentration for 30 min, oxidized at 230°C for 5 h, carbonized for 30 min.]

difference before and after immersion in the solution. The creatinine and VB_{12} concentrations of the solution were determined with a UV–Vis spectrophotometer (Shanghai Techcomp Corp. 7500) at wavelengths of 510 and 361 nm, respectively. Absorbency of creatinine and VB_{12} in the aqueous solutions reflects the difference of solution concentration. Then, the adsorption ratio was calculated as

$$\text{adsorption ratio (wt \%)} = \frac{\text{absorbency of before adsorption} - \text{absorbency of after adsorption}}{\text{absorbency of before adsorption}} \times 100\%$$

Samples of PAN-CHF and PAN-ACHF were characterized by measuring specific Brunaner–Emmett–Teller (BET) surface area and pore size distribution by using an auto-adsorption apparatus (Micromeritics Tristar 3000). The surface area was calculated by using the multipoint BET method. Pore volume and pore size distribution were determined from the nitrogen adsorption isotherms using the Barrett, Joyner, and Halenda (BJH) method.[19]

RESULTS AND DISCUSSION

Effect of carbonization temperature on the properties of PAN-CHF

Surface area and adsorption properties of PAN-CHF

Figure 2 shows the variation in burn-off and shrinkage ratio of PAN-CHF as a function of carbonization temperature of carbon hollow fibers. The weight loss and the shrinkage ratio were determined from a change in

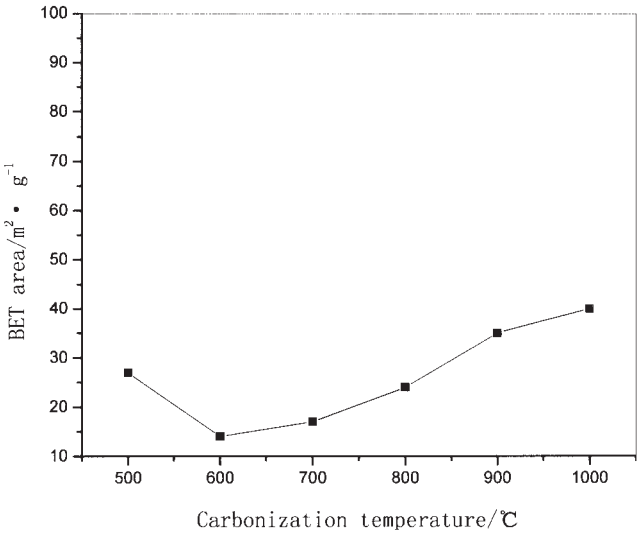

Figure 3 Specific surface area PAN-CHF versus carbonization temperature. [The samples are pretreated with ammonium dibasic phosphate of 4% (wt %) concentration for 30 min, oxidized at 230°C for 5 h, carbonized for 30 min.]

weight and length before and after carbonization. As shown in Figure 2, the weight loss of PAN-CHF gradually increases with carbonization temperature. The shrinkage ratio of PAN-CHF slowly increases with carbonization temperature and changes no more when carbonization temperature is 900°C. It is suggested that the weight loss of PAN-CHF is more easily changed by carbonization temperature than the shrinkage ratio. At elevated temperatures, the noncarbon elements are removed as volatiles (i.e., H_2O, HCN, NH_3, CO, CO_2, N_2, and so on) in the carbon fiber to give carbon fibers with weight loss and shrinkage.[20] The removal of volatiles from fibers becomes more drastic with carbonization temperature increasing so that the weight loss increases.

The specific surface areas for PAN-CHF have been plotted as a function of carbonization temperature in Figure 3. The specific surface areas increase as a whole with carbonization temperature. However, the surface areas of PAN-CHF prepared at different carbonization temperatures were below 40 $m^2\ g^{-1}$ as PAN-CHF was not activated with activated gas. During the carbonization stage, volatiles evolved and formed the carbon basal planes. Because the formation of carbon basal planes was due to the crosslinking reaction and the elimination of nitrogen,[21] the passage of the opened pores on the fiber surface was covered. Therefore, the defects between the basal planes on fiber surface were enveloped, and this reaction led to the decrease in surface area of the carbon fiber.

Figure 4 shows the variation in adsorption ratio of PAN-CHF as a function of carbonization temperature of carbon hollow fibers. The adsorption ratios to creatinine and VB_{12} are almost same before 800°C, then gradually increase, and change little at 900°C. However, the adsorption ratio to creatinine is higher than that to VB_{12} after 800°C, and the highest adsorption ratio to creatinine is about 90% and that to VB_{12} is about 75%. After the introduction of the paper, this means that there are basically micropores and not mesopores in PAN-CHF.

Morphology of PAN-CHF

Figure 5 shows the cross section of the PAN-CHF made of the fiber carbonized at 500, 700, and 900°C, respectively. The cross-sectional shape of CHF in Figure 5 (a–c), a difingerlike porous structure, is preserved after carbonization. It means that the carbonization process ulteriorly keeps the hollow shape of virgin hollow fiber and increasing carbonization temperature could not change the sectional shape of PAN-CHF more.

Effect of carbonization temperature on the properties of PAN-ACHF

Surface area and adsorption properties of PAN-ACHF

Figure 6 shows the variation in burn-off of PAN-ACHF and shrinkage ratio as a function of carbonization time of activated carbon hollow fiber. The weight loss and shrinkage ratio were determined from a change in weight and length before and after activation. The weight loss increases slowly before 800°C and then increases sharply. The shrinkage ratio changed little before 700°C and then increased slowly. Two reactions occurred simultaneously when the carbon fibers were heat treated during activation. One was the formation of new carbon basal planes, which

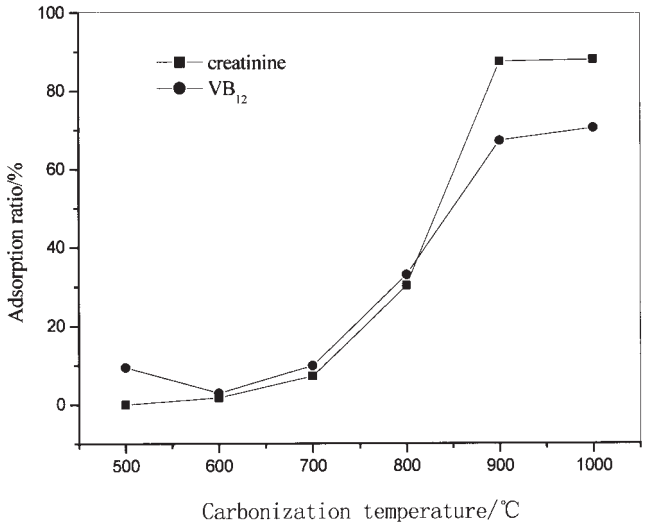

Figure 4 Adsorption ratio of PAN-CHF versus carbonization temperature. [The samples are pretreated with ammonium dibasic phosphate of 4% (wt %) concentration for 30 min, oxidized at 230°C for 5 h, carbonized for 30 min.]

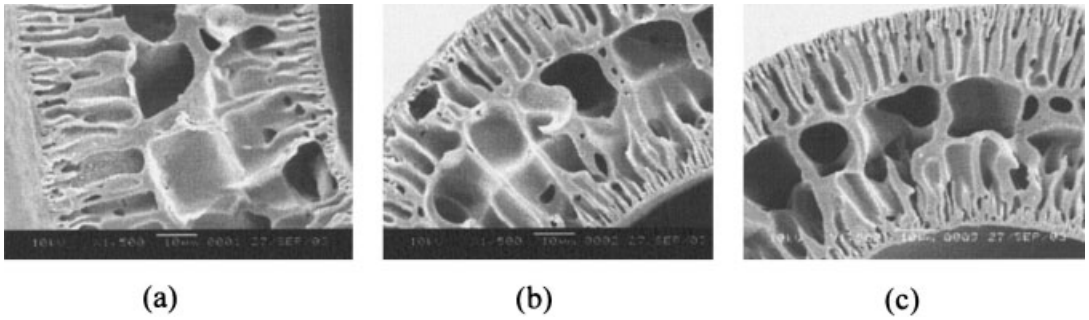

Figure 5 SEM micrographs of the cross sections of PAN-CHF (×1500). Carbonization temperature of a, b, c is 500°C, 700°C, 900°C. [The samples are pretreated with ammonium dibasic phosphate of 4% (wt %) concentration for 30 min, oxidized at 230°C for 5 h, carbonized for 30 min.]

led to a denser structure, and another was the degradation by carbon dioxide. When carbon fibers were heat treated in carbon dioxide, some structures of the fiber could be etched and removed. This reaction became more drastic and developed more pores with activation temperature increasing.

When the carbon fibers were heat treated during activation, two reactions occurred simultaneously. One was the formation of new carbon basal planes, which led to a denser structure, and another was the degradation by carbon dioxide at 880°C; some structures of the fiber could be etched and removed.[22,23] This reaction formed new pores. Figure 7 shows the variation in specific surface area of PAN-ACHF with carbonization temperature. The surface areas are low and increase slowly before 800°C and then sharply increase; a maximum surface area of 900 $m^2\ g^{-1}$ was found at 1000°C. By activating in CO_2 at high temperature, micropores and mesopores suitable for adsorption purpose would appear on the surface and the internal of PAN-ACHF. Ko et al.[24] found that the carbonization temperature for the precursor PAN fiber lower than the activation temperature produced the activated carbon fiber of the lowest surface area. In this work, as shown in Figure 7, the PAN-ACHF, made of the fiber carbonized at lower temperature (500°C, 600°C, 700°C, 800°C) than the activation temperature (900°C), had lower surface area, which was consistent with viewpoint of Ko et al. When the carbonization temperature (900°C, 1000°C) was equal to or higher than the activation time, the surface areas of PAN-ACHF, 620 and 900 $m^2\ g^{-1}$, respectively, were much higher than that made of the fiber carbonized at lower temperature.

Figure 8 shows the variation in adsorption ratio of PAN-ACHF as a function of carbonization temperature of activated carbon hollow fibers. The adsorption ratio to creatinine gradually increases with carbonization temperature and over 90%. The adsorption ratio

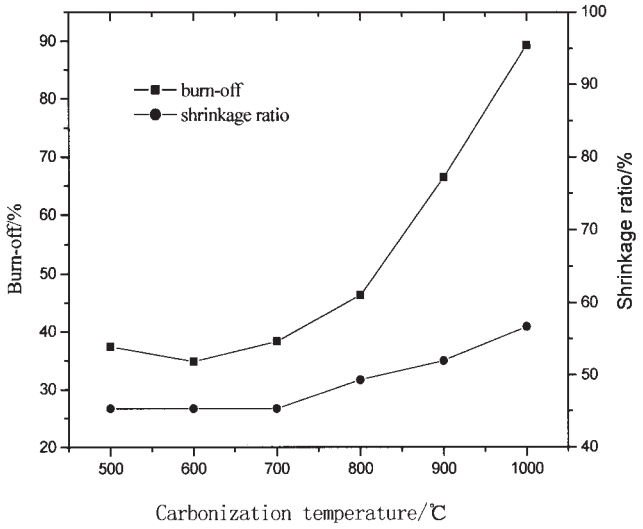

Figure 6 Burn-off and shrinkage ratio of PAN-ACHF versus carbonization temperature. [The samples are pretreated with ammonium dibasic phosphate of 4% (wt %) concentration for 30 min, oxidized at 230°C for 5 h, carbonized for 30 min, activated at 800°C for 40 min.]

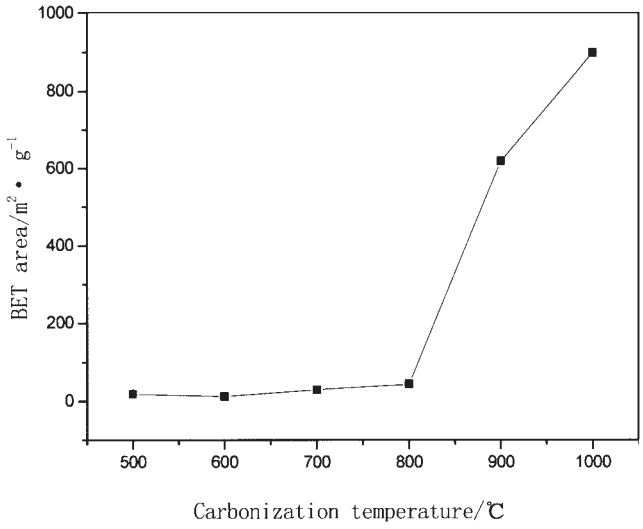

Figure 7 Specific surface area of PAN-ACHF versus carbonization temperature. [The samples are pretreated with ammonium dibasic phosphate of 4% (wt %) concentration for 30 min, oxidized at 230°C for 5 h, carbonized for 30 min, activated at 800°C for 40 min.]

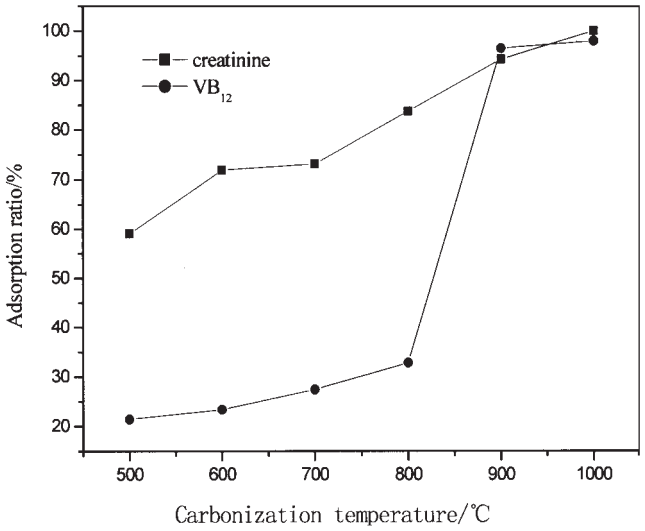

Figure 8 Adsorption ratio of PAN-ACHF versus carbonization temperature. [The samples are pretreated with ammonium dibasic phosphate of 4% (wt %) concentration for 30 min, oxidized at 230°C for 5 h, carbonized for 30 min, activated at 800°C for 40 min.]

to VB_{12} increases slowly before 800°C and then increases sharply and over 95% at 900°C. It is suggested that the number of micropores in PAN-ACHF increases with carbonization temperature, and the number of micropores and mesopores reaches a higher value after 900°C.

Pore size distribution of PAN-ACHF

Figure 9(a, b) shows the pore size distribution of the PAN-ACHF made of fiber carbonized at 900°C for 30 min. Due to the limits of apparatus, pore diameters of less than 2 nm could not be tested. However, the distribution of mesopores (2–50 nm) and macropores (>50 nm) can be observed by Figure 9(a, b). As shown in Figure 9, the pore volume of mesopores gradually decreases with average diameter when pore size is 2 to 5 nm, and correspondingly, incremental pore area decreases from 40 to 1 $m^2\ g^{-1}$ with average diameter. It indicates that the dominant pore sizes of mesopores in PAN-ACHF are from 2 to 5 nm. Moreover, a mass of micropores existed in PAN-ACHF and the amount of macropores is much less. So, the PAN-ACHF made of fiber carbonized at 900°C for 30 min has a high adsorption ratio to creatinine and VB_{12}, which is consistent with the conclusion of Figure 8.

Morphology of PAN-ACHF

Figure 10 shows the cross section and external surface of the PAN-ACHF made of the fiber carbonized at 500, 700, and 900°C, respectively, and then activated with carbon dioxide at 800°C for 40 min. The cross-sectional shapes of ACHF in Figure 10(a–c), difingerlike porous structure, is preserved after activation with CO_2 and similar. It means that CO_2 cannot diffuse deeper to cause activation in the depth of the hollow fiber when activation temperature is not more than 800°C. Micrograms in Figure 10(d–f) show the external surface of the resultant ACHF. For a carbonization temperature of 500 and 700°C, there are few pores, and white matter on the surface is unreacted phosphate, as shown in Figure 10(d, e). After 900°C of carbonization

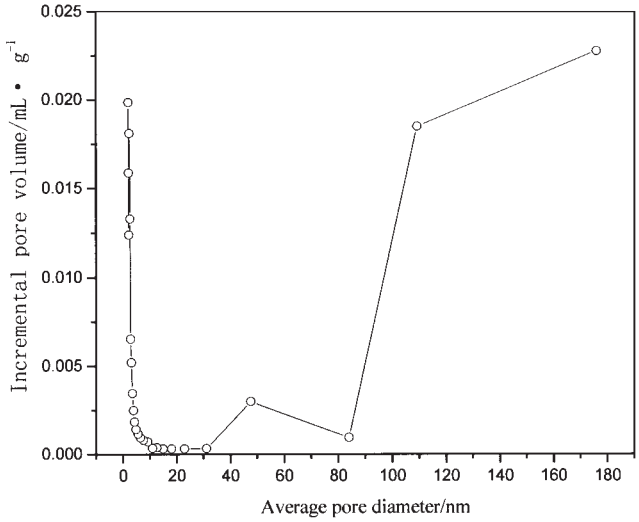

(a)

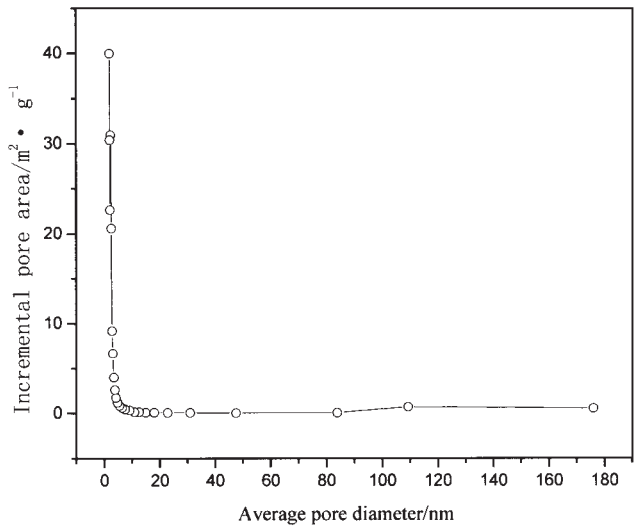

(b)

Figure 9 (a) The pore size distribution of PAN-ACHF. [The samples are pretreated with ammonium dibasic phosphate of 4% (wt %) concentration for 30 min, oxidized at 230°C for 5 h, carbonized at 900°C for 30 min, activated at 800°C for 40 min.] (b) The pore size distribution of PAN-ACHF. [The samples are pretreated with ammonium dibasic phosphate of 4% (wt %) concentration for 30 min, oxidized at 230°C for 5 h, carbonized at 900°C for 30 min, activated at 800°C for 40 min.]

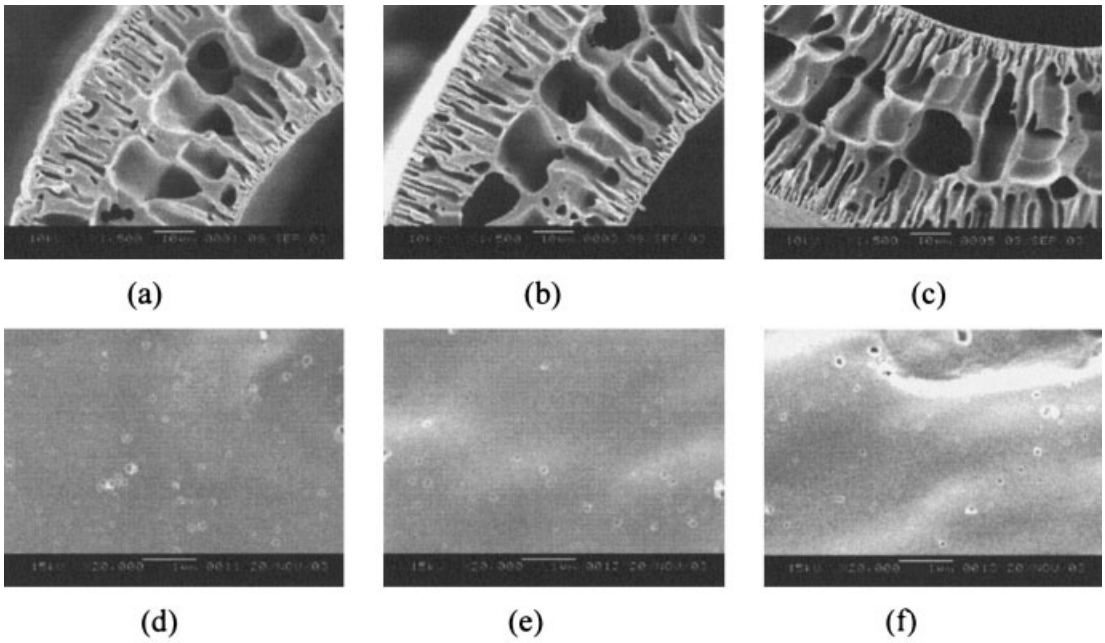

Figure 10 SEM micrographs of the cross sections (×1500) and external surface (×20,000) of PAN-ACHF carbonization temperature of a, b, c and d, e, f is 500°C, 700°C, 900°C, respectively. [The samples are pretreated with ammonium dibasic phosphate of 4% (wt %) concentration for 30 min, oxidized at 230°C for 5 h, carbonized for 30 min, activated at 800°C for 40 min.]

and 800°C of activation, pores began to increase on the surface and had uniform size, as shown in Figure 10(f). This suggests that the external surface and the thinner region of the skin of the hollow fiber have been activated, that the skin of the fiber was burned off, and that the molecules in the amorphous area were broken and the closed pores were opened.

CONCLUSIONS

The surface area of the carbon hollow fibers not activated with dioxide carbon is much lower. After the activation process, the surface area of the activated carbon hollow fibers increased very remarkably, reaching 900 $m^2\ g^{-1}$ when carbonization is 1000°C, and the adsorption ratios to creatinine and VB_{12} of ACHF were much higher than those of CHF, especially to VB_{12}. After the carbonization process and the activation process, the cross-sectional shape of CHF and ACHF, difingerlike porous structure, is preserved. Moreover, pores began to increase on the surface and had uniform size after 900°C of carbonization. The different adsorption ratios to two adsorbates including creatinine and VB_{12} reflect the number of micropores and mesopores in PAN-ACHF. The dominant pore sizes of mesopores in PAN-ACHF are from 2 to 5 nm.

References

1. Suzuki, M. Carbon 1994, 32, 577.
2. Fuertes, A. B.; Marban, G.; Munniz, J. Carbon 1996, 34, 223.
3. Fu, R.; Lu, H.; Zeng, H. Mater Res Soc Symp Proc 1994, 344, 88.
4. Suzuki, M. Water Sci Technol 1990, 23, 1649.
5. Saloda, A.; Suzuki, M.; Hirai, R.; Kawano, K. Water Res 1991, 25, 219.
6. Lu, Y.; Fu, R.; Chen, Y.; Zeng, H. Mater Res Soc Symp Proc 1994, 344, 83.
7. Komatsubara, Y.; Ida, S.; Fujitsu. H.; Mochida, I. Fuel 1984, 63, 1738.
8. Miyake, Y.; Suzuki, M. Gas Sep Purif 1993, 7, 229.
9. Arons, G. N.; Macnair, R.N.; Coffin, L. G.; Hogan, H. D. Textile Res J 1974, 44, 874.
10. Yang, M.-C.; Yu, D.-G. J Appl Polym Sci 1998, 58, 185.
11. Yang, M.-C.; Yu, D.-G. Textile Res J 1996, 66(2), 115.
12. Yang, M.-C.; Yu, D.-G. J Appl Polym Sci 1996, 69, 1725.
13. Yang, M.-C.; Yu, D.-G. J Appl Polym Sci 1996, 62, 2287.
14. Linkov, V. M.; Sanderson, R. D.; Jacobs, E. P. J Mater Sci 1994, 95, 93.
15. Linkov, V. M.; Sanderson, R. D.; Jacobs, E. P. Polymer Int 1994, 35, 239.
16. Mckinney, R., Jr. Desalination 1987, 62, 37.
17. Linkov, V.; Sanderson, R. D.; Jacobs, E. P. J Mater Sci Lett 1994, 13, 600.
18. Schindler, E.; Maier, F. U.S. Pat. 4,919,860, 1990.
19. Rist, L. P.; Harrison. D. P. Fuel 1985, 64, 291.
20. Donner, J.-B.; Bansal, R. C. Carbon Fibers; Marcel Dekker: New York, 1984; p 23.
21. Watt, W.; Johnson, D. J.; Parker, E. In Proceedings of the 2nd International Plastics Conference on Carbon Fibers; Plastics Institute: London, 1974; p 3.
22. Molleyre, F.; Bastick, M. In Proceedings of the 4th London International Conference on Carbon Graphite; Soc. Chem. Ind.: London, 1974; p 190.
23. Bahl, O. P.; Mathur, R. B.; Dhami, T. L. Polym Eng Sci 1984, 24, 455.
24. Ko, T. H.; Chiranairadul, P.; Lu, C. K.; Lin, C. H. Carbon 1992, 30, 647.